Mathematical determination of discrete sampling locations minimizing both the number of samples and the maximum interpolation error: application to measurements of surface ocean properties

Véronique Guglielmi[1], Franck Touratier[1], Catherine Goyet[1]

[1.] ESPACE-DEV, Univ Montpellier, IRD, Univ Antilles, Univ Guyane, Univ Réunion, Montpellier,France, IMAGES_ESPACE-DEV, Univ. Perpignan Via Domitia, Perpignan, France.
Veronique.guglielmi@univ-perp.fr; Franck.Touratier@univ-perp.fr; cgoyet@univ-perp.fr

This paper is a non-peer reviewed preprint submitted to EarthArxiv.

Mathematical determination of discrete sampling locations minimizing both the number of samples and the maximum interpolation error: application to measurements of surface ocean properties

Véronique Guglielmi[1], Franck Touratier[1], Catherine Goyet[1]

[1.] ESPACE-DEV, Univ Montpellier, IRD, Univ Antilles, Univ Guyane, Univ Réunion, Montpellier,France, IMAGES_ESPACE-DEV, Univ. Perpignan Via Domitia, Perpignan, France.

Abstract:

Over the past three decades, started extensive measurements of ocean properties at fixed stations throughout the water column, as well as in the surface ocean via oceanographic ships and via ships of opportunity. The later ones were particularly used to determine the air-sea CO_2 fluxes from automated measurements of sea-surface temperature, salinity, and CO_2 fugacity. These underway measurements, often recorded at a frequency of every minute, generate large data files that need to be quality controlled, stored and analyzed. Thus, for practical use, these data are often binned by 1° latitude x 1° longitude. Unfortunately, by doing so, there is loss of accuracy of these data sets.
Here, using the original 2010 underway data sets of sea-surface temperature, sea-surface salinity, total alkalinity and total inorganic carbon, along the cruise track from Hobart (Tasmania) to Dumont D'Urville (Antarctica), we show what would had been a more appropriate record pattern for each of these properties while still keeping the full accuracy of their measurements. Furthermore, we propose a general protocol to objectively determine appropriate locations of each property underway measurements according to their aimed accuracy. These results should greatly facilitate future cruise preparation and reduce cost of measurements, thus, our carbon imprint.

Keywords: Underway measurements, sampling strategy, interpolation error

1. Introduction:

In the actual context of global warming and increasing anthropogenic carbon dioxide into the atmosphere (Komhyr et al, 1989; Kirk et al., 1989; Keeling et al., 1996; Tans et al., 1996, Stephens et al., 2000; Hall et al., 2021; https://gml.noaa.gov/ccgg/trends/), there is a growing interest in quantifying the role of the ocean in the absorption of part of this atmospheric anthropogenic carbon (DeVries et al, 2014; Friedlingstein et al., 2020). Consequently, since a few decades, time-series stations and repeated transects of underway measurements (ICOS https://www.icos-cp.eu/; Dyfamed; http://www.obs-vlfr.fr/cd_rom_dmtt/sodyf_main.htm; HOT, BATS; https://scrippsco2.ucsd.edu/data/seawater_carbon/ocean_time_series.html), were designed to quantify the penetration of anthropogenic carbon in the ocean.

In the ocean, the anthropogenic carbon concentration cannot be measured. It has to be calculated from the measured total CO_2 concentrations (C_T, which include the natural and anthropogenic carbon) and various associated properties (such as temperature, salinity, total alkalinity, dissolved oxygen, etc.). Several approaches with various hypotheses exist (Brewer, 1978; Chen and Millero, 1979; Gruber et al, 1996; Goyet et al., 1999; Coatanoan et al., 2001; Touratier et al., 2004a,b; Lo Monaco et al., 2005; Touratier et al., 2007; Vazquez-Rodriguez et al., 2009). All of these numerous approaches were designed to compute anthropogenic carbon concentrations below the mixed layer depth down to the bottom (thus, they all assume to be in a closed system). Fortunately, generally, the results of most of these approaches provide relatively similar patterns (although their absolute values may differ and their accuracies are still debatable).

In the surface ocean (from the air-sea interface down to the depth of the wintertime mixed layer), many processes (such as air-sea exchanges [heat, gases, nutrients, etc.], mixing of water masses [fresh waters from rivers, surface currents, etc.], and seasonal biological activity), are at play. Thus, it is extremely difficult to disentangle the anthropogenic signal from the natural variations of total CO_2 concentrations (C_T).
At present, the only way to attempt to quantify the penetration of anthropogenic carbon in the surface ocean and to determine CO_2 sink and source areas of the ocean, is to assume the ocean is in quasi-steady-state (with negligible ocean circulation variation) and to perform repeated underway measurements. Thus, with the automatization of measuring systems (such as thermosalinographs for the Temperature and Salinity, or Infra-Red based instruments for CO_2 fugacity), it is possible to design programs based upon Ships of Opportunity (SOOP, https://community.wmo.int/ship-opportunity-programme), in addition to those based upon oceanographic research vessels.

In France, ships that supply the bases of the Terres Australes et Antarctique Française (TAAF), also provide an excellent opportunity to acquire such valuable data sets. Thus, several programs such as SURVOSTRAL (https://www.legos.omp.eu/survostral), and MINERVE (https://campagnes.flotteoceanogra-phique.fr/series/128/fr/), were designed to perform measurements of sea-surface temperature, salinity, CO_2 fugacity, total CO_2, and total alkalinity while the supply ship "L'Astrolabe" is underway between Hobart (Tasmania) and Dumont D'Urville (Terre Adélie, Antarctica).
Yet, after more than a few decades of sea-surface measurements, it is still very difficult to disentangle the anthropogenic signal from the natural signal. The seasonal and inter-

annual variations are still large compared with the anthropogenic perturbations (Laïka et al., 2009; Morrow and Kestenare, 2014 ; Brandon et al., 2022).

The objective of this work is to show how simple mathematical equations (based upon the general work of Davis and Goyet (2021)), can be used to determine an appropriate sea-surface sampling strategy adapted to each measurable property. The two main advantages of such sampling strategy are to minimize the number of data while increasing their interpolation accuracy, and to appropriately determine sample locations in high variability ocean areas.

2. Materials and methods

2.1. Data sets

Over the past few decades, the French Antarctic supply ship "*l'Astrolabe*" provided the opportunity to scientists to perform (mainly in austral summer), sea-surface measurements and sampling from Hobart, Tasmania (43°S 147°E) to the French Antarctic base Dumont D'Urville (66°S, 140°E).

As part of the SURVOSTRAL program (https://www.legos.omp.eu/survostral), continuous underway temperature and salinity "surface" seawater (at around 5 m), were measured since 1993 from R/V "*l'Astrolabe*" via a thermosalinograph (TSG). The raw data were recorded every minute. These raw data were then corrected for any biais (compared with discrete sample measurements), and by a median filter (over ± 12 minutes) to reduce the noise of the measurements. These raw and corrected data sets are freely available (https://sss.sedoo.fr; Alory et al., 2015). Below, we used the corrected data set.

Similarly, as part of the MINERVE program (https://campagnes.flotteoceanographique.fr/series/128/fr/), designed to quantify the interannual variability of the CO_2 properties in the Southern Ocean south of Tasmania, total alkalinity (A_T) and total CO_2 (C_T) were also sampled and measured from R/V "*l'Astrolabe*". These data are freely available (https://data.ifremer.fr/SISMER).

For the purpose of this work, we are focusing only the transect Hobart – Dumont D'Urville which occurred in February 19-23, 2010. The choice of this transect was randomly picked among the transects where Total alkalinity (A_T) and Total CO_2 (C_T) were measured.

The measurements accuracy of sea-surface salinity (SSS), during this 2010 cruise is estimated to be ± 0.005 (Morrow and Kestenare, 2014). The measurements accuracy of sea-surface temperature (SST), is estimated to be ± 0.001°C (from the manufacturer). The measurements accuracy of total alkalinity (A_T) and total CO_2 (C_T) measurements are estimated to be ± 3,5 $\mu mol.kg^{-1}$ and ± 2,7 $\mu mol.kg^{-1}$, respectively (similar to the accuracies of these measurements performed on board previous MINERVE cruises [Laïka et al, 2009]).

Figure 1 shows the result of the measurements of these four properties (SST, SSS, A_T, C_T) along the cruise track from Hobart (Tasmania) to Dumont D'Urville (Antarctica), in February 2010. These graphs clearly show the disparity in the frequency of the measurements. There are 7815 data points for SST and SSS (one every minute; N = 7815 for SST and SSS), while there are only 238 data points for A_T and C_T (due to the difficulty and time of measurements; N = 238 for A_T, C_T).

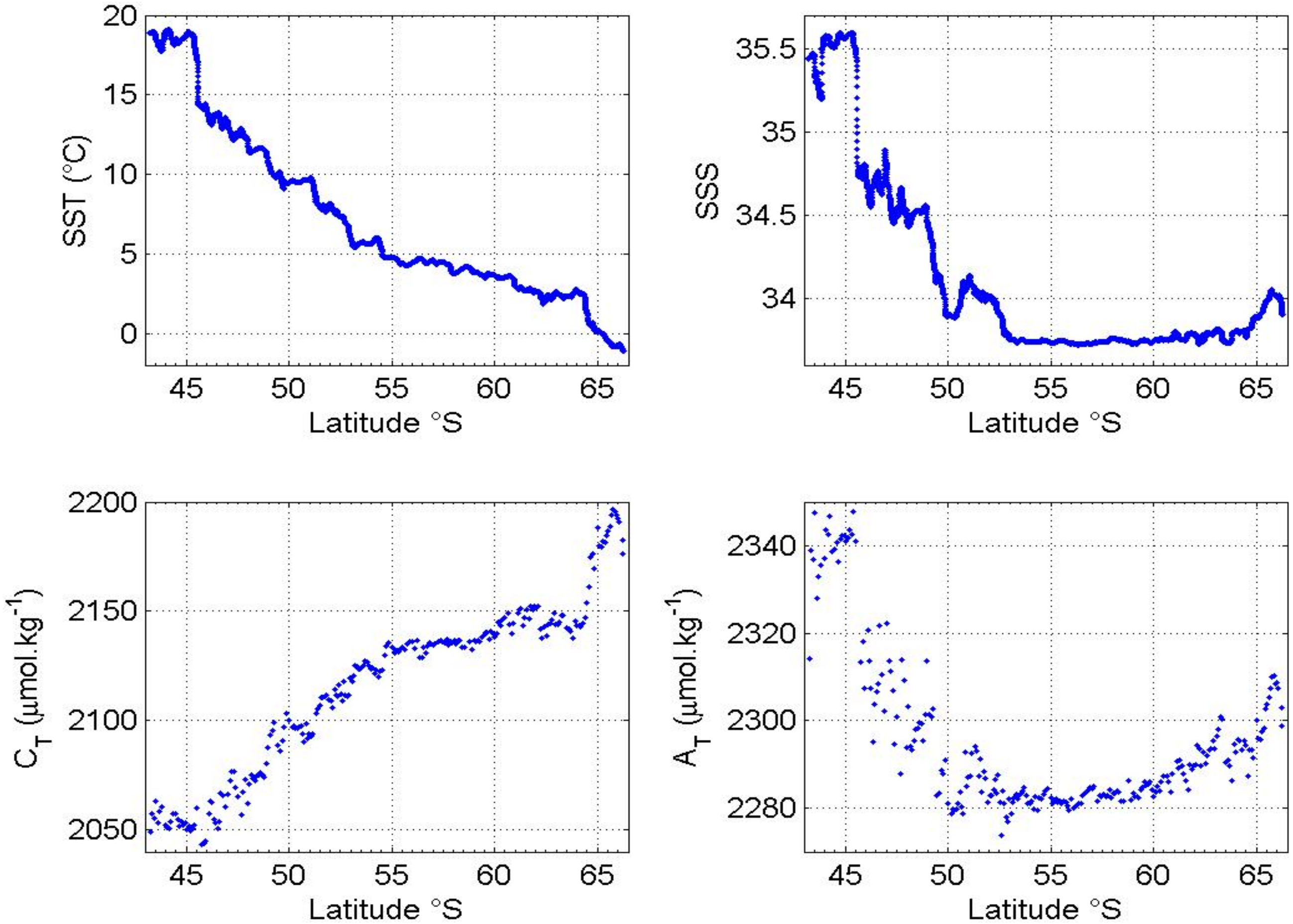

Fig.1 Measured property as a function of latitude; a) SST and b) SSS measured every minute (7815 measurements), c) C_T and d) A_T measured roughly every 20 minutes (238 measurements).

2.2. Method

Based upon the work of Davis and Goyet (2021), who showed for example, how to determine appropriate Total CO_2 (C_T) sampling pattern throughout a water column from the surface to the bottom, we will use the same equations to show how they can be used to determine appropriate sampling patterns for underway surface ocean measurements of SST, SSS, A_T and C_T.

Here, we first remind the main principle and equations (which are explained and demonstrated in details in Davis and Goyet, 2021), and then we use the 2010 data to provide a concrete illustration of proper application of these equations to determine appropriate sampling patterns for each of the four properties (SST, SSS, A_T and C_T).

Main principle and mathematical equations for optimizing underway measurements

Briefly, the principle of this method (Davis and Goyet, 2021), is to find a mathematical equation to determine the error function as a function of the space and variability functions. Since the variability function depends upon the signal itself (which cannot be changed), the error function can be minimized only by adjusting the space function.

Considering a signal Y as a function of X, the first step is to determine the signal variability and its bounds.
By definition, the signal variability (VarY(X)), can be calculated as follows:

$$\mathrm{VarY(X)} = 2 * ([\,\Delta^{+}Y / \Delta^{+}X\,] - [\,\Delta^{-}Y / \Delta^{-}X\,]) / (\Delta^{+}X + \Delta^{-}X) \qquad (1)$$

with $\Delta^{+}Y = Y_{i+1} - Y_i$; $\Delta^{-}Y = Y_i - Y_{i-1}$; $\Delta^{+}X = X_{i+1} - X_i$; $\Delta^{-}X = X_i - X_{i-1}$; for i= 2, …,N-1
where the first "i" starts at the second measured point, up to the one before last.

In other words, the signal variability is similar to the second derivative of the signal.

The maximum of the bound (*BndY(X)*) of this signal variability is noted *MaxBndY(X).*

Consequently, the maximum error of interpolation of a regular sampling pattern of N samples points in the interval [*XsI, XeI*] is given by the relationship (Davis and Goyet (2021):

$$\mathrm{MaxErrEven}(N, MaxBndY(X), XsI, XeI) = \left(\frac{MaxBndY(X)}{8}\right) . \left(\frac{(XeI - XsI)}{(N-1)}\right)^2 \qquad (2)$$

The maximum error of interpolation of a balanced error sampling pattern (irregular sampling pattern), is given by the relationship (Davis and Goyet, 2021):

$$\mathrm{MaxErrBal}(N, XsI, XeI) = (1/[8\,(N-1)^2]) \cdot \left(\int_{XsI}^{XeI} \sqrt{BndY(X)}\, \mathrm{d}X\right)^2 \qquad (3)$$

It is also possible to calculate the number of samples needed to reach an aimed maximum error (MaxErrY) within a given interval [*XsI* , *XeI*], where there is a constant bound (CstBnd) of its signal variability.

For samples regularly spaced along the X axis, the number of samples needed can be calculated from the relationship (Davis and Goyet, 2021):

$$\mathrm{SampleSizeEven}(\mathrm{MaxErrY}, \mathrm{Cst}Bnd, XsI, XeI) = (XeI - XsI) . \sqrt{\frac{\mathrm{Cst}Bnd}{8 * \mathrm{MaxErrY}}} + 1 \qquad (4)$$

For samples regularly spaced along the Y axis (irregularly spaced along the X axis), the number of samples needed can be calculated from the relationship (Davis and Goyet, 2021):

$$\text{SampleSizeBal}(\text{MaxErrY}, XsI, XeI) = \frac{\int_{XsI}^{XeI} \sqrt{BndY(X)}\, dX}{\sqrt{8 * MaxErrY}} + 1 \quad (5)$$

The sample positions in an interval where the balanced error sampling pattern is chosen can be determined as follows (Davis and Goyet, 2021):
Given a strictly increasing function A(x): $A(x) = \int_a^x \sqrt{BndY(t)}\, dt$ in an interval [a, b], the following function calculates the distribution of the samples such as the values of studied property are regularly spaced:

$$Distribute(M, A(x)) = \{x_i\ i=0,\ldots, M-1,\ x_0 = a \leq x_i \leq b = x_{M-1}\} \quad (6)$$

Such that $A(x_{i+1}) - A(x_i) = (A(b) - A(a))/(M-1)$, with i = 0, …, M-1.
Where M represents the number of points to be distributed within the interval [a, b].

In other words, instead of distributing the samples points regularly along the X axis, they are distributed regularly along the Y axis.

3. Results and discussion for underway SST and SSS measurements

During the 2010 cruise, the SST and SSS properties were measured and recorded along with the ship's position (latitude and longitude) every minute. Since the ship was mainly sailing southward, and at a more or less constant speed, we will consider that the "x" axis is only the latitude (L).

Since the TSG instrument measurement error for the temperature and salinity can be estimated as ± 0.001°C and ± 0.005, respectively, we would aim for an interpolation maximum error of half that of the measurements. Thus, we define MaxErrT = ± 0.0005°C and MaxErrS = ± 0.0025, for SST and SSS, respectively. Consequently, the overall uncertainty of the interpolated data along the whole cruise track would be less than (0.001 + 0.0005) ± 0.0015°C for temperature and (0.005 + 0.0025) ± 0.0075 for salinity.

In practice the temperature and salinity errors can be higher (Morrow and Kestenare, 2017), if one takes into account the environmental errors in addition to the instruments errors. Thus, below, the results will be shown for the three aimed MaxErrT **(**± 0.0005°C; ± 0.005°C ; ± 0.05°C) and three MaxErrS (± 0.0025; ± 0.005; ± 0.01).

3.1 Determination of the temperature and salinity variabilities and their bounds

Figure 2 illustrates each SST variability (VarT(L)) and SSS variability (VarS(L)), respectively, as calculated according to eq.1, as well as their respective bounds (*Bnd*T(L) and *Bnd*S(L)). Thus, the chosen points (latitude, temperature) for the temperature variability bounds are:
*Bnd*T(L) = {(43.2262, 16600), (46, 16600), (52, 10545), (53.5, 4500), (63, 4500), (64.1, 6940), (66.2598, 6940)},

and similarly, the chosen points (latitude, salinity) for the salinity variability bounds are: *Bnd*S(L) = {(43.2262, 3260), (44, 3260), (45.3, 1000), (45.5, 2000), (46.8, 2000), (46.91, 55000), (46.98, 5500), (47, 1800), (52, 1800), (53.5, 400), (60, 400), (62, 900), (65.5, 900), (65.7, 1900), (65.8, 1900), (66.2598, 700)}.

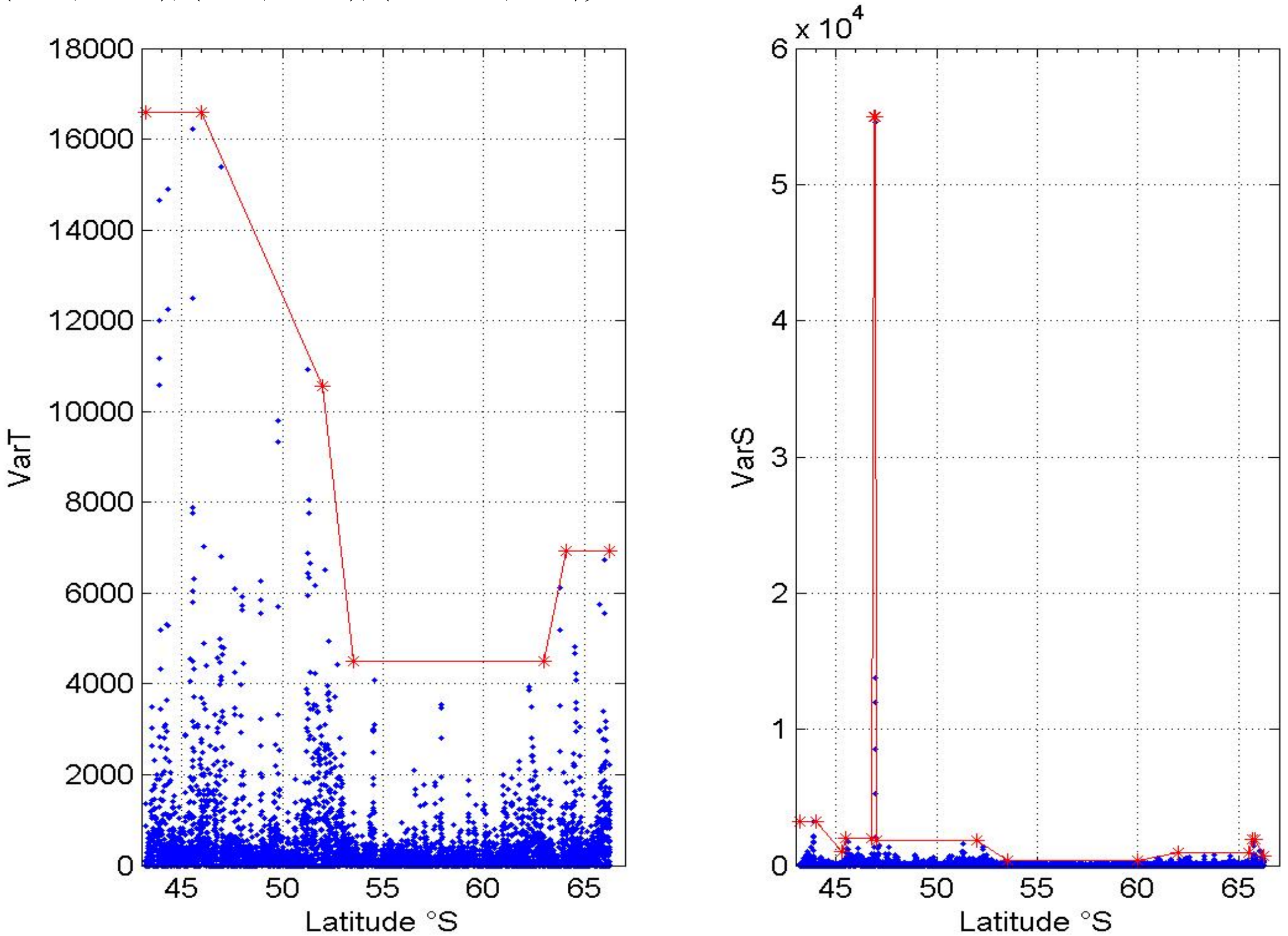

Figure 2. Variability of a) sea-surface temperature, and b) sea-surface salinity, as a function of latitude (in decimal degree). The solid (red) lines on each graph represents the variability bounds.

Figure 2 clearly shows that the temperature and salinity bounds have different shapes and thus, it may not be appropriate to measure them simultaneously. This observation is also in good agreement with the results, based upon vertical temperature and salinity data, presented in Davis and Goyet (2021). Consequently, in order to minimize the number of measurements in the ocean (from the surface seawater throughout the bottom waters), while insuring the highest accuracy of each property, SST and SSS measurements should be performed at different locations.

For instance, here, as illustrated in Fig.2, there is a large difference between the SST and SSS variabilities at latitudes near 47°S. There is a huge salinity variability while the temperature variability is decreasing. As shown in figure 3, these differences in variabilities reflect the differences in the SST and SSS signals.

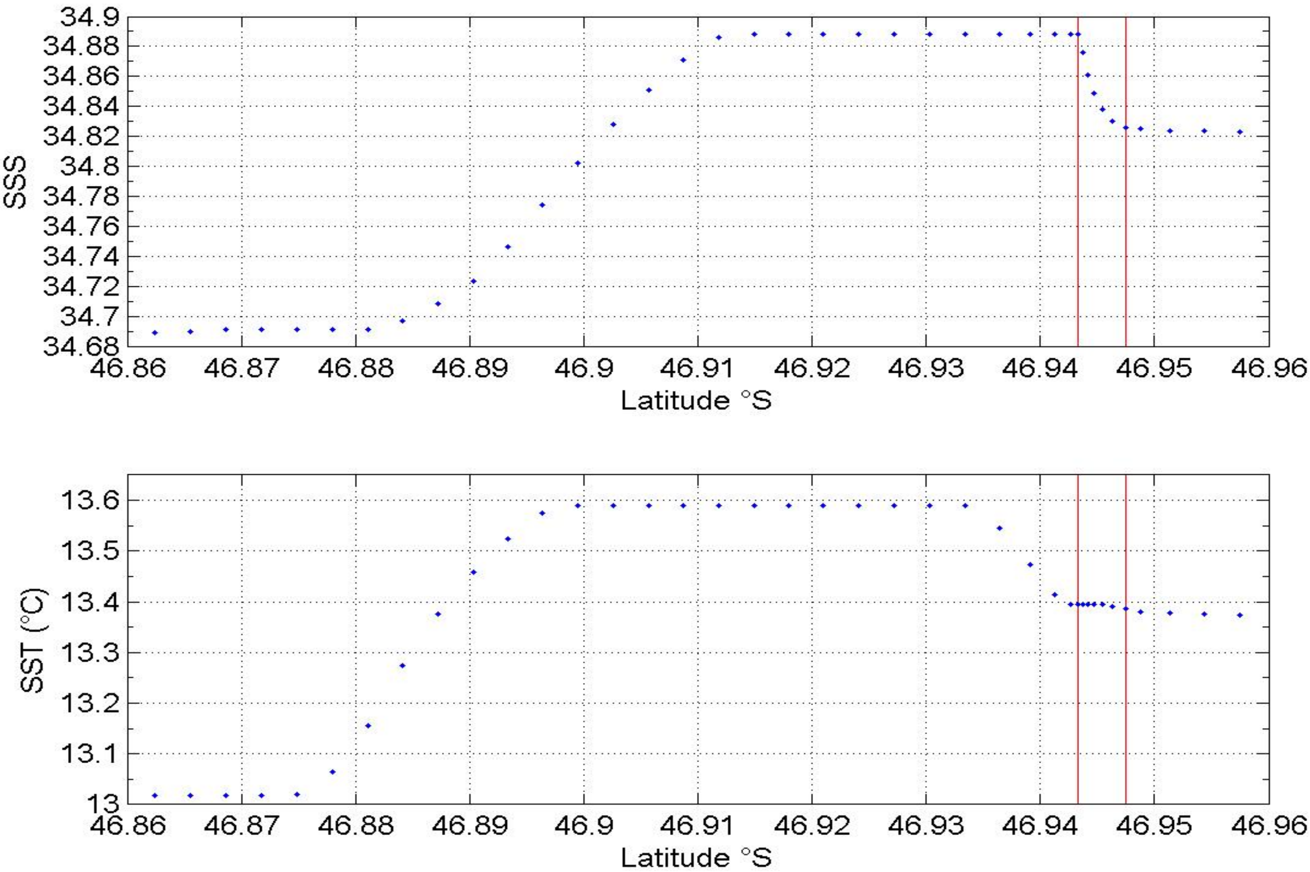

Figure 3. Zoom of the SSS and SST data within the latitude interval [46,86°S ; 46,96°S].

This figure 3, which is zoom of figure 1 within the latitude interval [46,86°S; 46,96°S], clearly shows that both the increase and the decrease in temperature and salinity occur at different latitudes, with a latitude shifted around 0,01° (about 1 km), and at a very different rate. Such features are typical of fine surface ocean structures. Thus, they are expected to occur within this ocean area, especially between the SubTropical Front (STF), and the SubAntarctic Front (SAF) where there are many eddies, cold cores, and filaments with important SST and SSS small scales variations.

Inside such fine structures (below meso-scale), SSS and SST vary on different time scales. In general SST varies much faster than SSS due to air-sea interactions. This was clearly illustrated in a previous study by Morrow et al., (2004). They showed that the fronts signatures of minimum of SSS and SST in cold cores are significantly sharper for SSS than for SST. In their discussion, Morrow et al., (2004), indicated: "Our summer XBT and TSG observations show that these cold-core eddies quickly lose their surface SST signature; generally, a few weeks of summer warming removes the cooler SST signature (we cannot be more precise due to the temporal resolution of our sampling). The fresher SSS is a better indicator of these subsurface cold-core eddies, and the surface salinity signature can last for one or 2 months after the ring detachment."

In another time-series study, Morrow and Kestenare (2014) further illustrated the recurrent high SSS variability in this ocean area in particular near 47°S and South of the STF.

3.2 Determination of the temperature and salinity maximum interpolation errors

For temperature measurements along the cruise track from 43.2262°S to 66.2598°S, the result of eq.2 for an even sampling pattern is MaxErrEven(SST) = 0.018°C and that of eq.3 for a semi-balanced error sampling pattern is MaxErrBal(SST) = 0.009°C. Thus, these results indicate that:

1) either it is unnecessary to use a temperature probe as accurate as 0.001°C since the interpolation accuracy cannot be better than 0.018°C. Thus, a temperature probe with an accuracy of 0.036°C would suffice for an even sampling pattern for an overall (measurement + interpolation) accuracy of 0.054°C, or a temperature probe with an accuracy of 0.018°C would suffice for a balanced error sampling pattern for an overall (measurement + interpolation) accuracy of 0.027°C.
2) or it is necessary to greatly increase the frequency of the measurements to keep the overall uncertainty below 0.0015°C,
3) or it may be appropriate to use a higher order interpolation (Davis and Goyet, 2021).

For salinity measurements along the cruise track from 43.2262°S to 66.2598°S, the result of eq.2 for an even sampling pattern is MaxErrEven(SSS) = 0.0597 and that of eq.3 for a semi-balanced error sampling pattern is MaxErrBal(SSS) = 0.0013. Thus, these results indicate that:

1) either it is unnecessary to use a salinity probe as accurate as 0.005 since the interpolation accuracy cannot be better than 0.0597. A salinity probe with a measurement accuracy of 0.12 would suffice for an even sampling pattern for an overall (measurement + interpolation) accuracy of 0.18.
2) or it is necessary to increase the frequency of the measurements to keep the overall uncertainty below 0.0075,
3) or it is necessary to use a semi-balanced error sampling strategy which will provide an interpolation error of only 0.0013 (below le aimed maximum interpolation error of 0.0025), for an overall (measurement + interpolation) accuracy of 0.0063. Thus, in this case, it would be possible to reduce the number of measurements performed.
4) or in order to further reduce the number of measurements it may be appropriate to use a higher order interpolation (Davis and Goyet, 2021).

In other words, these results indicate that for SST, a more efficient sampling pattern would be a semi-balanced error sampling pattern. Yet, it will be necessary to considerably increase the number of measurements to reach an aimed maximum interpolation error below 0.005°C. In any case, SST sampling would be regularly spaced along the latitudinal axis when the variability remains constant in the three latitude intervals [43.2262°S – 46°S], [53,5°S – 63°S], [64,1°S – 66,2598°S]. And sampling would be irregularly spaced along the latitudinal axis when the variability varies in the three intervals [46°S – 52°S], [52°S – 53,5°S], [63°S – 64,1°S].

Similarly, these results show that for SSS, a more efficient sampling pattern would be a semi-balanced error sampling pattern. But contrary to SST, it would be possible to reduce the number of measurements to reach the aimed maximum interpolation error below 0.0025, if they were appropriately (irregularly) spread along the cruise track.

In order to determine more appropriate sampling patterns for SST and SSS, it is necessary to calculate the number of samples needed prior to determine their locations.

3.3 Determination of the number of sample needed to reach the aimed accuracy using even and balanced error sampling patterns

Since it is appropriate to use an even sampling pattern in areas where the bounds of the variability signal are constant, and to use a balanced error sampling pattern in areas where the bounds of the variability signal varies, the calculated number of samples needed for SST and SSS along the cruise track (depending upon the aimed accuracy), between Hobart and Dumont D'Urville can be calculated using eq. 4 and 5. The results are summarized in Table 1 for measurements of SST and in Table 2 for measurements of SSS.

Latitudinal interval	N measured	Aimed SST Maximum interpolation error		
		0.0005°C	0.005°C	0.05°C
43.2262°S - 46°S	905	5652	1788	566
46°S - 52°S	2015	11030	3489	1104
52°S - 53.5°S	566	2044	647	205
53.5°S - 63°S	3109	10077	3187	1009
63°S - 64.1°S	357	1314	416	132
64.1°S - 66.2598°S	863	2846	901	285
43.2262°S - 66.2598°S	7815	32958	10423	3297

Table 1. Numbers of samples needed within each latitudinal interval to reach the aimed maximum interpolation error for SST measurements. The gray boxes indicate that the number of samples are calculated (using eq.5) for a semi-balanced sampling pattern. The white boxes indicate that the number of samples are calculated (using eq.4) for an even sampling pattern.

Remark: In these tables the number of samples calculated over the whole latitudinal interval (last line in the tables) are less than the sum of samples within the sub-intervals. This is due to rounding of the result (since a fraction of a sample would be meaningless), and of the limits (ex: one sample at 52°S would be counted twice; once in the interval [46°S; 52°S] and once in the interval [52°S; 53.5°S]).

It is clear from these results (Table 1), that the aimed SST maximum interpolation error of 0.0005°C is far from being reached with "only" 7815 measurements (quasi-evenly spaced), since it would require a minimum of 32958 measurements (more than 4 times 7815 points) judiciously located along the cruise track. The aim of maximum interpolation error of 0.005°C could not even be reached with the 7815 measurements (which represent a measurement every minute), since it would need at least 10423 data.

On the other hand, if the maximum interpolation error needed were of only 0.05°C, then 7815 measurements would be more than twice too many since only 3297 measurements would suffice.
As expected, it is in the latitude interval [53.5°S; 63°S], where the SST variability is the lowest, that the number of samples measured (3109) is the closest (per degree of latitude), to the one calculated (3187) for an aimed maximum interpolation error of 0.005°C.

Table 2 illustrates that to reach the SSS aimed maximum interpolation error of 0.0025 the number of measurements could be significantly reduced if they were performed at key locations rather than evenly spaced. Using a semi-balanced pattern strategy, only 5527 measurements would suffice while the 7815 measurements evenly spaced are not enough to reach the aimed maximum interpolation error of 0.0025. Furthermore, if the aimed maximum interpolation error is set to only 0.05, the number of SSS measurements needed would drop down to 3908 (a reduction by a factor close to 2 of the 7815 measurements).

Latitudinal interval	N measured	Aimed SSS Maximum interpolation error		
		0.0025	0.005	0.01
43.2262°S - 44°S	253	313	222	157
44°S - 45.3°S	432	420	297	210
45.3°S - 45.5°S	60	56	40	28
45.5°S - 46.8°S	432	412	292	207
46.8°S - 46.91°S	36	126	90	64
46.91°S - 46.98°S	30	117	83	59
46.98°S - 47°S	7	24	17	12
47°S - 52°S	1670	1501	1062	751
52°S - 53.5°S	566	346	245	174
53.5°S - 60°S	2137	920	651	461
60°S - 62°S	646	359	254	180
62°S - 65.5°S	1155	743	526	372
65.5°S 65.7°S	71	54	38	27
65.7°S -65.8°S	63	32	23	16
65.8°S - 66.2598°S	257	117	83	59
43.2262°S - 66.2598°S	7815	5527	3908	2764

Table 2. Numbers of samples needed within each latitudinal interval to reach the aimed maximum interpolation error for SSS measurements. The gray boxes indicate that the number of samples are calculated (using eq.5) for a semi-balanced sampling pattern. The white boxes indicate that the number of samples are calculated (using eq.4) for an even sampling pattern.

Overall, these results indicate that today, temperature and salinity data recorded every minute along a cruise track do not guarantee linear interpolation errors less than half that of these accurate measurements. They also emphasize the fact that the SSS and SST variabilities may significantly differ in time and space. Thus, it would be best if SSS and SST be measured at different rate to preserve their respective measurement accuracies. This would further avoid over sampling, and consequently would reduce our carbon imprint (consumption of energy [measurements and data analysis], data analysis [quality control, …, storage], etc.).

These results further indicate that lowering the expected accuracy would considerably reduce the required frequency of the measurements. Thus, it would be judicious to assure that the objectives in term of interpolation errors could be reached with the given accuracy of the measuring systems.

In practice, it may not be possible (or desirable if scientists do not wish to study cold cores, eddies, or filaments), to considerably increase the frequency of measurements when there is a very sharp variability variation of a property (such as that observed for salinity near 47°S). In such case, it may be appropriate to feint to ignore this localized very high variability to determine reasonable variability bounds over the whole signal.

For example, in this case for salinity we could define the variability bounds as:
*Bnd*S(L) = {(43.2262, 3260), (44, 3260), (45.3, 1800), (52, 1800), (53.5, 400), (60, 400), (62, 900), (65.5, 900), (65.7, 1900), (65.8, 1900), (66.2598, 700)}. These bounds are shown in figure 4.

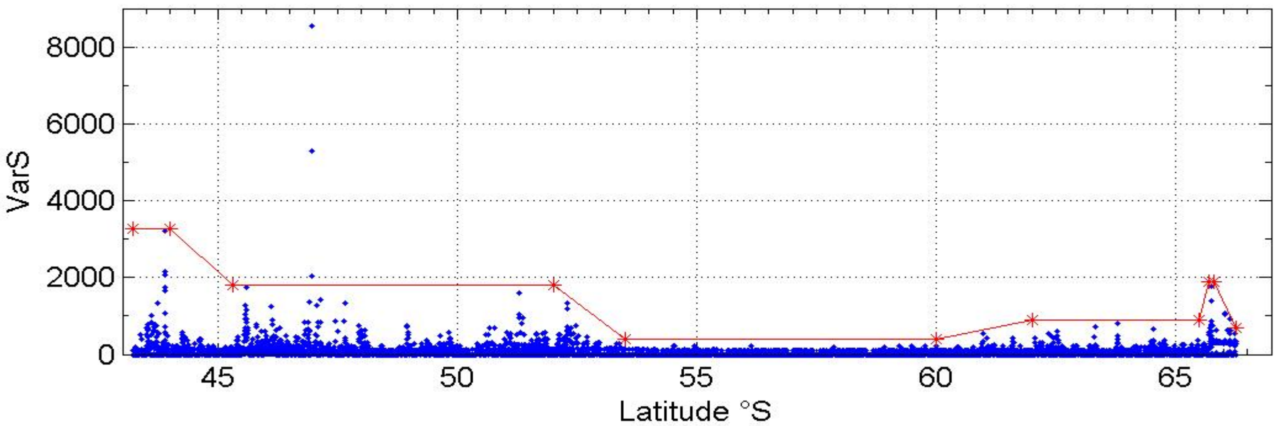

Figure 4. Variability of sea-surface salinity as a function of latitude. The red lines represent the variability bounds if the highest SSS variability is ignored.

With these new bounds, using eq.2 MaxErrEven(SSS) = 0.0354 and using eq.3 MaxErrBal(SSS) = 0.0012. Compared with the ones above (MaxErrEven(SSS) = 0.0597; MaxErrBal(SSS) = 0.0013), these results, clearly illustrate the importance of the choice of a variability bound. The closest, such bound is to a variability signal, the lowest is the number of samples needed to recover the full signal (with a minimum interpolation error). As expected, these results further show that the largest difference is with an even sampling pattern. Thus, there is always a significant advantage to use a semi-balanced error sampling pattern, to minimize the number of measurements while ensuring a lowest interpolation error.

Using these new bounds, the results of the sample size needed in each latitudinal interval are summarized below in Table 3.

Latitudinal interval		Aimed SSS Maximum interpolation error

	N measured	0.0025	0.005	0.01
43.2262°S - 44°S	253	313	222	157
44°S - 45.3°S	432	462	327	231
45.3°S - 52°S	2235	2011	1422	1006
52°S - 53.5°S	566	346	245	174
53.5°S - 60°S	2137	920	651	461
60°S - 62°S	646	359	254	180
62°S - 65.5°S	1155	743	526	372
65.5°S 65.7°S	71	54	38	27
65.7°S -65.8°S	63	32	23	16
65.8°S - 66.2598°S	257	117	83	59
43.2262°S - 66.2598°S	7815	5349	3783	2675

Table 3. Numbers of samples needed within each latitudinal interval to reach the aimed maximum interpolation error for SSS measurements assuming the high SSS variability near 47°S does not exist. The gray boxes indicate that the number of samples are calculated (eq.5) for a semi-balanced sampling pattern. The white boxes indicate that the number of samples are calculated (eq.4) for an even sampling pattern.

Table 3 illustrates that without taking into account the high variability near 47°S, to reach the SSS aimed maximum interpolation error of 0.0025 the number of measurements could be reduced to 5349. This a reduction of 178 measurements compared with the number of measurements needed (5527, Table 2) to take into account the full SSS variability.

Furthermore, as expected, if the aimed maximum interpolation error is set to only 0.05, the number of SSS measurements needed would drop down to only 3783 (a reduction of only 125 measurements compared with result [3908] in Table 2). As the expected maximum interpolation error increases, the number of measurements decreases and lesser is the effect of moving the variability bounds.

Then, knowing the number of measurements needed in each latitude interval, it is easy to determine their positions. In areas where the variability bound is constant, the measurements would be regularly spaced, while in areas where the variability bound is variable, the position of measurements would be simply determined using eq.6.
Remark: here, since the function BndY(t) is a simple linear function (a*t + b), the integral of its square-root can be calculated exactly;
$\int_{t1}^{t2} \sqrt{(a*t+b)}$ dt = $(a * t2 + b)^{3/2} * 2/(3*a) - (a * t1 + b)^{3/2} * 2/(3*a)$. However, if the function BndY(t) were more complex, the integral could simply be done numerically.

Given the relatively high number of data, a figure of the results of eq.6 would not help to visualize them. Thus, we choose to show the results of eq.6 only for the A_T and C_T sampling (below) which are considerably less numerous.

4. Results and discussion for underway A_T and C_T measurements

Since the accuracy of the total alkalinity and total CO_2 concentrations are 3.5 µmol.kg^{-1} and 2.7 µmol.kg^{-1}, respectively, for both properties, we would aim to an interpolation accuracy of half the accuracy of the measurements. Thus, we define MaxErrA$_T$ = 1.75 µmol.kg^{-1} and MaxErrC$_T$ = 1.35 µmol.kg^{-1}.

4.1 Determination of the A_T and C_T variability bounds

Figure 5 illustrates the variabilities and their bounds for total alkalinity and total CO_2 data.

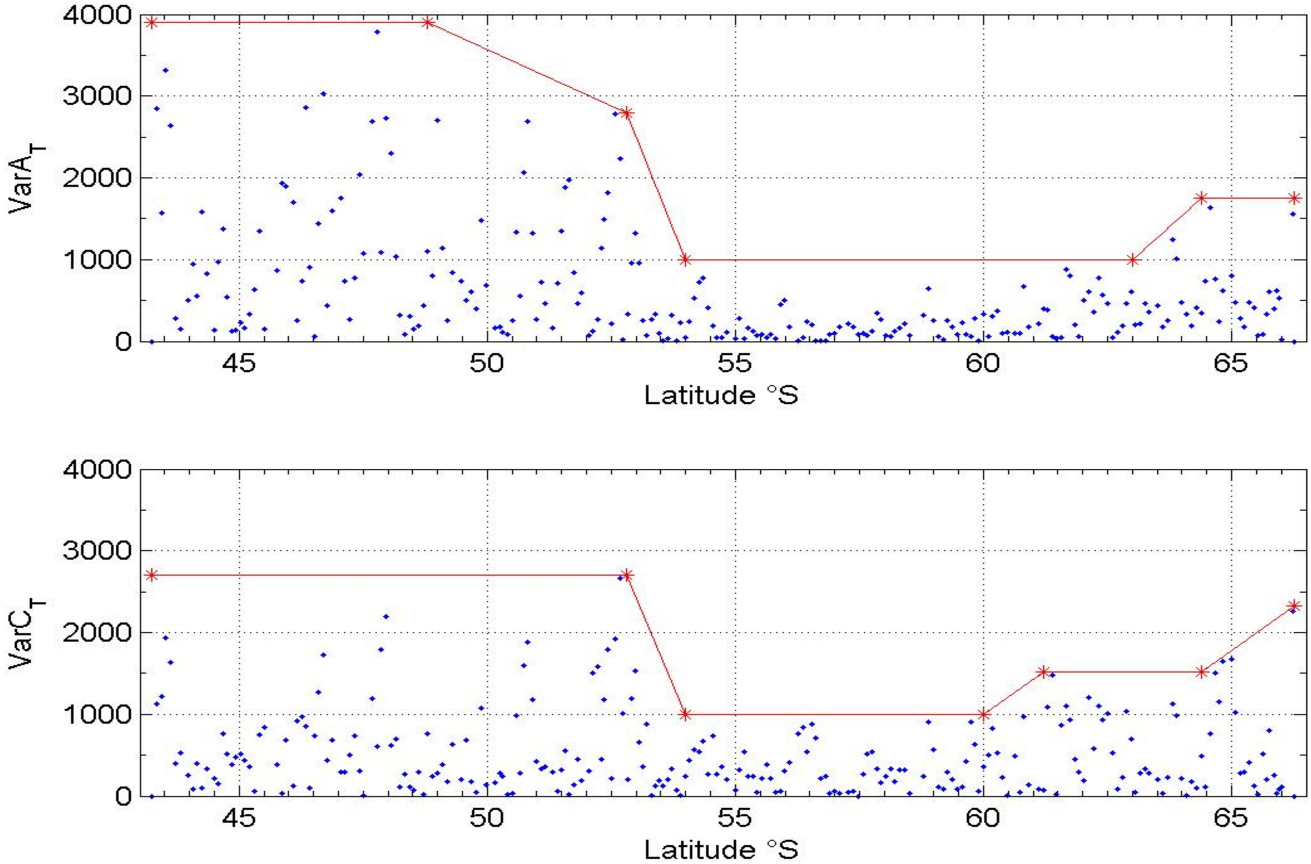

Figure 5. Variability of a) total alkalinity as a function of latitude, and b) total inorganic carbon as a function of latitude. The solid (red) lines on each graph represent the variability bounds.

Consequently, the chosen points (latitude, A_T) for the A_T variability bounds (reported in Figure 5) are:
BndA$_T$(L) = {(43.25, 3900), (48.8, 3900), (52.8, 2800), (54, 1000), (63, 1000), (64.4, 1750), (66.25, 1750)}, and the chosen points (latitude, C_T) for the C_T variability bounds (reported on Figure 5) are:
BndC$_T$(L) = {(43.25, 2700), (52.8, 2700), (54, 1000), (60, 1000), (61.2, 1520), (64.4, 1520), (66.25, 2320)}.

Figure 5 further shows that the A_T and C_T bounds do not have the same shape. Thus, knowing the maximum of variability ($MaxBndA_T$ = 3900 for T, and $MaxBndC_T$ = 2700 for

C_T), the maximum errors of interpolation of these data sets with 238 points, can be easily calculated using eq. 2 and 3. The results along the cruise track (43.25°S - 66.25°S) are: MaxErrEven(A_T) = 4.59 µmol.kg^{-1} ; MaxErrEven(C_T) = 3.18 µmol.kg^{-1}; MaxErrBal(A_T) = 2.42 µmol.kg^{-1} ; MaxErrBal(C_T) = 2.16 µmol.kg^{-1}.

Since the results for both (an even pattern sampling or an irregular sampling pattern), indicate a maximum interpolation error larger than the aimed interpolation error (±1.75 µmol.kg^{-1} for A_T and ±1.35 µmol.kg^{-1} for C_T, as mentioned above), it is clear that 238 samples evenly spaced along the latitude axis between Hobart and Dumont D'Urville are not enough. These results clearly show that the position of the samples have a significant impact on the interpolation accuracy.

Given the acquired knowledge on the A_T and C_T variability bounds, it is now possible to design an appropriate sampling strategy with a minimum of samples. Thus, where the bound is constant, samples will be evenly spaced along the latitudinal axis, and in areas where the bound varies, samples will be unevenly spaced along the latitudinal axis.

In order to determine the exact position of samples to be measured throughout the cruise track, it is necessary to first determine the number of samples to be taken (depending upon the aimed maximum interpolation error), within each latitudinal area defined by the variability bound, and then to calculate the sample positions in the areas where the variability bound varies.

Tables 4 and 5 illustrate the results of the sample size needed (calculated using eq. 4 and eq.5), in each latitudinal interval for A_T and C_T, respectively. These Tables further show the results of the calculation performed for three aimed maximum interpolation error. The first one guided by our effective cruise measurement accuracies. The second and third ones assume the measurements are performed with an improved accuracy of 2 µmol.kg^{-1} and 1 µmol.kg^{-1}, respectively. Note that these improved targeted accuracies are reasonable and reachable.

Latitudinal interval	N measured	Aimed A_T Maximum interpolation error		
		0.5 µmol/kg	1.0 µmol/kg	1.75 µmol/kg
43.25°S - 48.8°S	55	174	124	94
48.8°S - 52.8°S	43	117	83	63
52.8°S - 54°S	15	27	19	15
54°S - 63°S	90	143	102	77
63°S - 64.4°S	14	27	19	15
64.4°S - 66.25°S	21	40	28	22
43.25°S - 66.25°S	238	523	370	280

Table 4. Numbers of samples needed within each latitudinal interval to reach the aimed maximum interpolation error for A_T measurements. The gray boxes indicate that the number of samples are calculated (eq.5) for a semi-balanced sampling pattern. The white boxes indicate that the number of samples are calculated (eq.4) for an even sampling pattern.

For total alkalinity, the results (Table 4) indicate that the aimed maximum interpolation error of 1.75 µmol.kg^{-1} was reached within the two latitudinal intervals [54°S, 63°S] and [64.4°S, 66.25°S] since in these intervals 77 and 22 samples respectively, are needed while during the cruise 90 and 21 samples were effectively measured in these intervals, respectively. In the interval [52.8°S, 54°S], the aimed maximum interpolation error could have been reached only IF the 15 measured samples would have been measured according to a semi-balanced error sampling pattern (unevenly spaced along the latitudinal axis). Within the remaining three intervals ([43.25°S, 48.8°S], [48.8°S, 52.8°S], [63°S, 64.4°S]), they were not enough samples to reach the aimed maximum interpolation error of 1.75 µmol.kg^{-1}.

These results further show the significant increase in the number of samples needed as the aimed maximum interpolation error decreases.

For total inorganic carbon, the results (Table 5) indicate that the aimed maximum interpolation error of 1.35 µmol.kg^{-1} can be reached only within the latitudinal interval [54°S, 60°S]. All the other latitudinal intervals need to be sampled at a higher rate. This is logic since the aimed maximum interpolation error is reduced compared with that of A_T. Here too, the results reported in Tables 4 and 5, clearly show the significant differences in the number of samples needed as the aimed maximum interpolation error decreases.

Latitudinal interval	N measured	Aimed C_T Maximum interpolation error		
		0.5 µmol/kg	1.0 µmol/kg	1.35 µmol/kg
43.25°S - 52.8°S	98	249	177	152
52.8°S - 54°S	15	26	19	16
54°S - 60°S	59	96	68	59
60°S - 61.2°S	11	22	16	13
61.2°S - 64.4°S	34	63	45	39
64.4°S - 66.25°S	21	41	29	25
43.25°S - 66.25°S	238	494	350	301

Table 5. Numbers of samples needed within each latitudinal interval to reach the aimed maximum interpolation error for C_T measurements. The gray boxes indicate that the number of samples are calculated (eq.5) for a semi-balanced sampling pattern. The white boxes indicate that the number of samples are calculated (eq.4) for an even sampling pattern.

Since the shape of the A_T variability bound is different from that of the C_T variability bound, ideally their sampling patterns would be different. However, as mentioned above, for various reasons (technique of measurement, convenience, …), it may be required or desirable, to collect samples simultaneously for A_T and C_T measurements. In this case, it is then necessary to define a combined bound.

A common variability bound for A_T and C_T can be calculated as follows (Davis and Goyet, 2021):

$$Bnd\mathrm{A_TC_T}(L) = \max\left([Bnd\mathrm{A_T}(L)/minBnd\mathrm{A_T}],\ [Bnd\mathrm{C_T}(L)/minBnd\mathrm{C_T}]\right) \quad (7)$$

Where “L” represents the latitude, *minBnd*A_T represents the minimum of the A_T variability bound, and *minBnd*C_T represents the minimum of the C_T variability bound.

Then the combined bound for each of the A_T and C_T property can be determined as:

$$\mathrm{Comb}Bnd\mathrm{A_T(L)} = minBnd\mathrm{A_T} \ * \ Bnd\mathrm{A_TC_T(L)} \quad (8)$$

and

$$\mathrm{Comb}Bnd\mathrm{C_T(L)} = minBnd\mathrm{C_T} \ * \ Bnd\mathrm{A_TC_T(L)} \quad (9)$$

Note : Since in this particular case *minBnd*A_T = *minBnd*C_T, then the combined limits Comb*Bnd*A_T(L) and Comb*Bnd*C_T(L) will be identical.

Consequently, here, the combined bounds (reported in figure 6) are:
Comb*Bnd*A_T(L) = Comb*Bnd*C_T(L) = {(43.25, 3900), (48.8, 3900), (52.8, 2800), (54, 1000), (60, 1000), (61.2, 1520), (63, 1520), (64.4, 1750), (66.25, 2320)}.

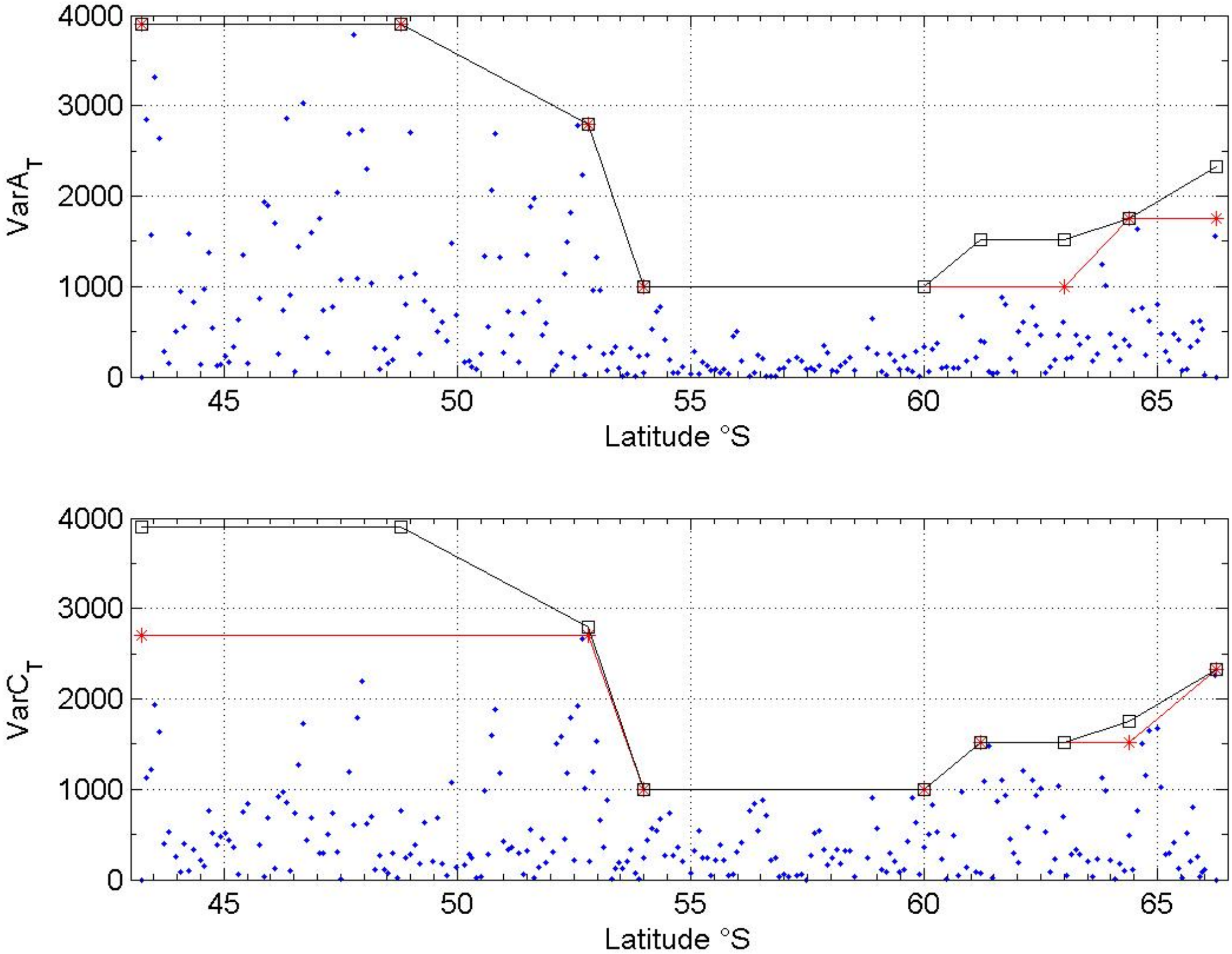

Figure 6. Variability of a) total alkalinity as a function of latitude, and b) total inorganic carbon as a function of latitude. The red lines with the stars on each graph represent the variability bounds (as above in fig. 5), and the black lines with the open squares represent the combined variability bounds.

Using these combined bound, the results (eq.2&3) are: MaxErrEven = 4.59 μmol.kg^{-1} and MaxErrBal = 2.56 μmol.kg^{-1}.

As expected these results clearly show that 238 samples (evenly spaced or not) along the latitude axis [43.25°S - 66.26°S] between Hobart and Dumont D'Urville are not enough to reach the aimed maximum interpolation error.

Consequently, in order to determine the minimum number of samples required to reach the aimed maximum interpolation error of 1.35 µmol.kg^{-1} for C_T (as well as A_T), it is necessary to calculate the number of samples within each latitudinal zone defined by the combined variability bounds. The results are illustrated in Table 6.

Latitudinal interval	N measured	Aimed A_T or C_T Maximum interpolation error		
		0.5 µmol/kg	1.0 µmol/kg	1.35 µmol/kg
43.25°S - 48.8°S	55	174	124	106
48.8°S - 52.8°S	43	117	83	71
52.8°S - 54°S	15	27	19	17
54°S - 60°S	59	96	68	59
60°S - 61.2°S	11	22	16	14
61.2°S - 63°S	20	36	26	22
63°S - 64.4°S	14	29	21	18
64.4°S - 66.25°S	21	43	30	26
43.25°S - 66.25°S	238	537	380	327

Table 6. Numbers of samples needed within each latitudinal interval to reach the aimed maximum interpolation error for A_T and C_T measurements. The gray boxes indicate that the number of samples are calculated (eq.5) for a semi-balanced sampling pattern. The white boxes indicate that the number of samples are calculated (eq.4) for an even sampling pattern.

Since, in this case sample locations are identical for A_T and C_T measurements, the aimed maximum interpolation error has to be the smallest of two. Thus, here, it will be 1.35 µmol.kg^{-1}, that of C_T measurements.

These results show that in order to reach the aimed maximum interpolation error of 1.35 µmol.kg^{-1}, for A_T and/or C_T measurements along this cruise track between 43.25°S and 66.25°S, it would be necessary to collect at least 327 samples at specific locations, while only 238 samples were measured at quasi-regularly spaced locations along the latitude axis. Thus, in some areas, such as within the interval [54°S; 60°S], the location and number of samples measured were sufficient, while in other areas, such as within the interval [43.25°S; 48.8°S], the number of samples measured is clearly not enough (by almost a factor 2). Yet in other areas, such as within the intervals [52.8°S; 54°S] and [60°S; 61.2°S], the number of samples measured is close to sufficient but only IF they would have been measured at appropriate irregular spacing locations.

In order to provide further insights on the number of samples required as the aimed accuracy improves, and assuming it is possible to perform the A_T and C_T measurements with an accuracy of 2.00 µmol.kg^{-1} or 1.00 µmol.kg^{-1}, the same calculation was performed for an aimed maximum interpolation error of 1.00 µmol.kg^{-1}, and 0.50 µmol.kg^{-1}. The results are also reported in Table 6. They show that the number of samples measured would need to be increased significantly (from 327 to 380, to 537) as the interpolation error decreases (from 1.35 µmol.kg^{-1} to 1.00 µmol.kg^{-1}, and 0.50 µmol.kg^{-1}, respectively).

In summary, in order to reach an aimed maximum interpolation error for both A_T and C_T, measurements along this cruise track, an appropriate sampling strategy would be to first determine the number of samples needed within each interval and then to sample regularly along the latitude ("x") axis within the three intervals [42.25°S – 48.8°S], [54°S – 60°S] and [61.2°S – 63°S], and to distribute the samples according to eq.6 within the following five other areas [48.8°S – 52.8°S], [52.8°S – 54°S], [60°S – 61.2°S], [63°S – 64.4°S] and [64.4°S – 66.25°S].

For example, for an aimed maximum interpolation error of 1.35 µmol.kg^{-1}, figure 7 illustrates the results of the function A(x) = $\int_a^x \sqrt{BndY(t)}$ dt (eq.6) with "x" within the latitudinal interval [52.8°S – 54°S]. The 17 samples needed in this latitudinal interval are then regularly distributed along the A(x) ("y") axis to find the position of the samples on the latitude ("x") axis.

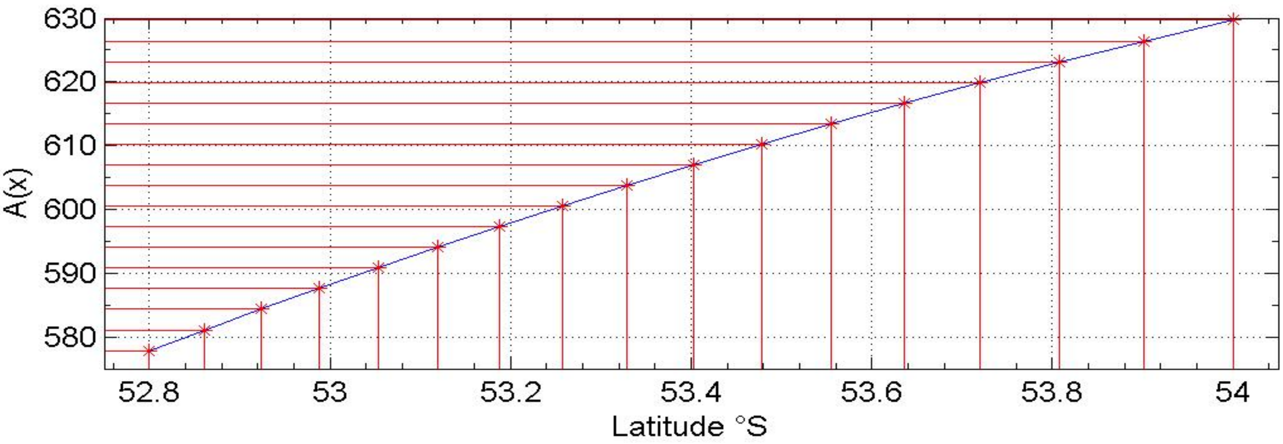

Figure 7. Function A(x) = $\int_a^x \sqrt{BndY(t)}$ dt within the latitude interval [52.8°S – 54°S].

This figure clearly shows that within the 0.2° latitudinal interval [52.8°S – 53°S] four samples would be needed, while within the other 0.2° latitudinal interval [53.8°S – 54°S], only three samples would be needed. Thus, with this function, an appropriate irregular spacing between samples can be easily calculated.

Figure 8 shows the result (of eq.6) for an appropriate number of samples and their positions within the interval [43.25°S; 66.25°S], to reach an aimed maximum interpolation error of 1.35 µmol.kg^{-1}, for both A_T and C_T.

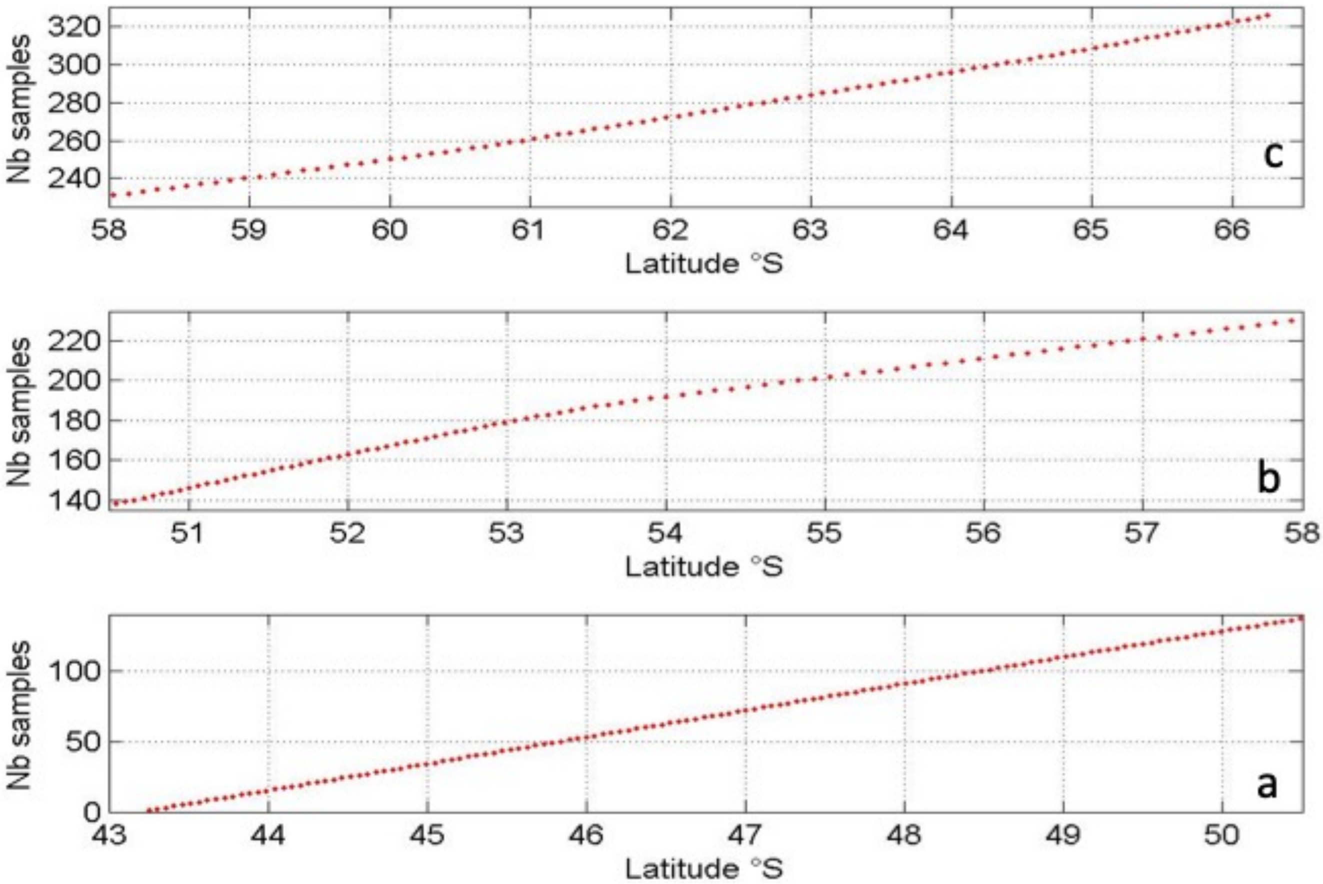

Figure 8. Sample location for each of the 327 samples within the latitudinal interval [43.25°S; 66.25°S]. In order to best visualize the position of the samples, the figure is split in three areas; a) [43.25°S; 50.5°S], b) [50.5°S; 58°S], and c) [58°S; 66.25°S].

This figure 8 illustrates that spacing between samples should vary from very small in the area [43.25°S; 48°S], to much larger in the area [54°S; 60°S], and to relatively small South of 60°S. The number of samples required within each degree of latitude is shown in figure 9.

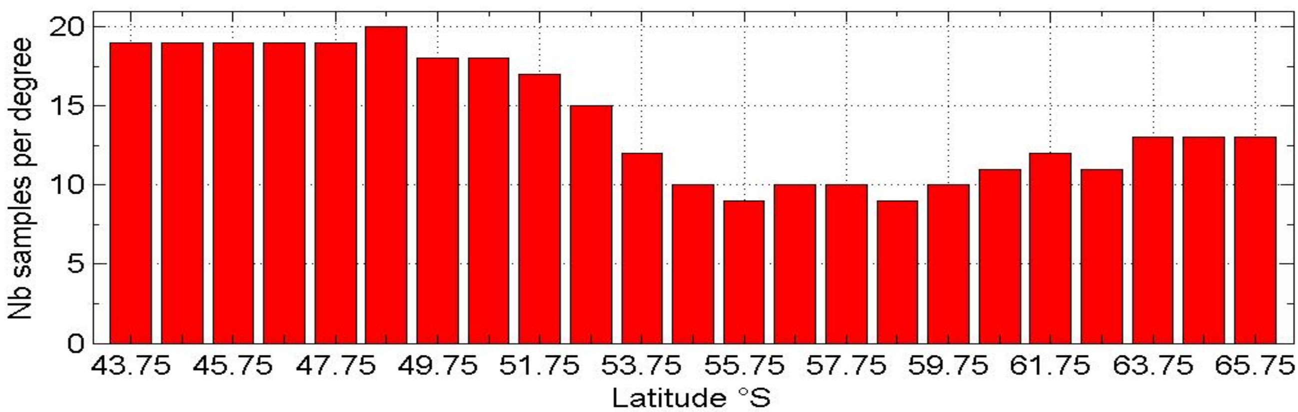

Figure 9. Number of samples per degree of latitude within the interval [43.25°S ; 66.25°S]

Thus, these two figures (8 and 9) clearly illustrate that the property variability bound determines the relative proportion of samples spread over the latitudinal interval ('x' axis). Where the property variability is high, the number of samples should be high.

Where the property variability is constant, the samples should be regularly spaced, as illustrated in fig.9 by the same number of samples per degree of latitude at the beginning and at the end of the cruise track. Where the property variability bounds vary, the number of sample per degree varies (see Fig.8 and 9, within the latitudinal areas [50°S; 55°S] and [58°S; 62°S]).

5. Conclusions

This study shows that with simple calculations, it is possible not only to know the maximum linear interpolation error of any measured property, but also to precisely determine the positions of these measurements along a cruise track (based upon previous data sets) while minimizing both the number of these measurements and the maximum interpolation error.

Since the accuracy of each property measurement depends upon the measuring system, each property would be ideally measured on its proper sampling pattern. However, if for any (practical) reason, two (or more) properties should be sampled simultaneously, then it is possible to determine a common sampling pattern. Such common pattern will increase the number of measurements required to preserve the aimed maximum interpolation error of each of these properties.

All these calculations are based upon the variability of the signal or more exactly upon the bounds of the property variability. In areas where the variability bounds of a property (such as here, SST, SSS, A_T, or C_T), are constant, sampling would ideally be regularly spaced along the 'x' axis (here, the "latitude" axis). However, in areas where the variability bounds are variable, sampling would ideally be irregularly spaced along the "x" axis and would tend to be regularly spaced along the property axis, such that the maximum error between samples remains quasi-constant (whatever the amplitude of property variability).

The choice of the variability bounds of a property is particularly important since all the calculations are based upon them. In order to make sure to catch the whole signal variability, it is good to define large variability bounds, but that means that the property would probably be oversampled. On the other hand, if the variability bounds are chosen too short, there will be less samples to measure but with the risk of missing the highest signal variability. Thus, depending upon the objectives priorities and various practical constraints, one would have to find an equilibrium between sample size and accuracy.

The key factor to design an appropriate sampling strategy (with a minimum of samples/measurements), is to know both, the accuracy of the measurements and the aimed maximum interpolation error.

In any case, all the results as presented above for SSS, SST, A_T, and C_T, show that the current sampling strategy can significantly be improved by using a semi-balanced interpolation error sampling strategy.

In particular, this study emphasizes the large difference in the number of SSS and SST measurements needed (5527 and 32958, respectively), along a cruise track between Hobart and Dumont D'Urville, to ensure that the maximum interpolation errors remain below half the property measurement accuracy. Concerning A_T, and C_T, "only" 327 measurements could be sufficient. Even if it can be assumed that A_T, and C_T can be measured with an improved accuracy of 1 µmol.kg^{-1}, "only" 380 measurements could be sufficient. Yet, this would still represent a significant effort since a measurement of A_T and/or C_T usually take much more time and is much more expensive than a SSS or SST measurement.

Why is there such a large difference between the A_T and/or C_T and SSS number of measurements? As mentioned above, all the calculations are based upon the estimate of the property variability bounds. Since the number of SSS data is large (7815), all short-scale SSS variabilities (such as that near 47°S), are likely to be detected, thus raising the maximum of the bound. On the other hand, since the number of A_T and/or C_T data is relatively small (238), some short-scale variabilities may remain undetected, thus lowering the maximum variability bound.

These results further raise the question of scientific need for measurements accuracies, the number and location of the measurements needed, as well as which scientific questions could be answered with the present technology. Or, what kind of new technologies are needed to make significant scientific progresses?
For instance, here, one could conclude that there is an urgent need to develop new reliable technologies for much faster (and cheaper) measurements of A_T and C_T in seawater.

Overall, this study based upon simple equations (in section 2.2), significantly facilitate the determination of appropriate sampling and measurement locations, even when the number of measurements is limited by various constraints (time, cost, technology, accuracy, etc.). These equations are general and can be applied to any kind of environmental studies (geology, meteorology, etc.), with any kind of data (in situ, remotely sensed, etc.). Thus, this study opens the route to more efficient sampling strategies (and cruise designs), which will enhance scientific progress.

Acknowledgments:
We genuinely thank Alain Poisson for the initiation of the MINERVE program, as well as Elodie Kestenare and Rosemary Morrow for the SURVOSTRAL data and helpful comments.
We are grateful to Daniel Davis for helpful discussions, thoughtful suggestions, and providing language help.
We thank the Terres Austral et Antactique Françaises (TAAF) and the Institut Paul Emile Victor (IPEV) for logistic support during the 2010 cruise.

Funding:
This research did not receive any grant from funding agencies in the public, commercial, or not-for-profit sectors.

References:

Alory, G., Delcroix, T., Téchiné, P., Diverrès, D., Varillon, D., Cravatte, S., Gouriou, Y., Grelet, J., Jacquin, S., Kestenare, É., 2015. The French contribution to the voluntary observing ships network of sea surface salinity. Deep Sea Research Part I: Oceanographic Research Papers 105, 1–18.

Brandon M., C. Goyet, F. Touratier, N. Lefèvre, E. Kestenare, R. Morrow, 2022. Spatio-temporal variability of the CO_2 properties and anthropogenic carbon penetration, in the Southern Ocean surface waters. Deep Sea Research Part I: Oceanographic Research Papers

Brewer, P.G., 1978. Direct observation of the oceanic CO_2 increase. Geophysical Research Letters 5, 997–1000.

Chen, G.-T., Millero, F.J., 1979. Gradual increase of oceanic CO_2. Nature 277, 205–206.

Coatanoan, C., Goyet, C., Gruber, N., Sabine, C.L., Warner, M., 2001. Comparison of two approaches to quantify anthropogenic CO_2 in the ocean: Results from the northern Indian Ocean. Global Biogeochemical Cycles 15, 11–25.

Davis, D., C. Goyet 2021. Balanced Error Sampling: With application to ocean biogeochemical sampling. Presses Universitaires de Perpignan. 224pp.

DeVries, T., 2014. The oceanic anthropogenic CO_2 sink: Storage, air-sea fluxes, and transports over the industrial era. Global Biogeochem. Cycles 28, 631–647. https://doi.org/10.1002/2013GB004739

Friedlingstein, P., O'Sullivan, M., Jones, M.W., Andrew, R.M., Hauck, J., Olsen, A., Peters, G.P., Peters, W., Pongratz, J., Sitch, S., Le Quéré, C., Canadell, J.G., Ciais, P., Jackson, R.B., Alin, S., Aragão, L.E.O.C., Arneth, A., Arora, V., Bates, N.R., Becker, M., Benoit-Cattin, A., Bittig, H.C., Bopp, L., Bultan, S., Chandra, N., Chevallier, F., Chini, L.P., Evans, W., Florentie, L., Forster, P.M., Gasser, T., Gehlen, M., Gilfillan, D., Gkritzalis, T., Gregor, L., Gruber, N., Harris, I., Hartung, K., Haverd, V., Houghton, R.A., Ilyina, T., Jain, A.K., Joetzjer, E., Kadono, K., Kato, E., Kitidis, V., Korsbakken, J.I., Landschützer, P., Lefèvre, N., Lenton, A., Lienert, S., Liu, Z., Lombardozzi, D., Marland, G., Metzl, N., Munro, D.R., Nabel, J.E.M.S., Nakaoka, S.-I., Niwa, Y., O'Brien, K., Ono, T., Palmer, P.I., Pierrot, D., Poulter, B., Resplandy, L., Robertson, E., Rödenbeck, C., Schwinger, J., Séférian, R., Skjelvan, I., Smith, A.J.P., Sutton, A.J., Tanhua, T., Tans, P.P., Tian, H., Tilbrook, B., van der Werf, G., Vuichard, N., Walker, A.P., Wanninkhof, R., Watson, A.J., Willis, D., Wiltshire, A.J., Yuan, W., Yue, X., Zaehle, S., 2020. Global Carbon Budget 2020. Earth Syst. Sci. Data 12, 3269–3340. https://doi.org/10.5194/essd-12-3269-2020

Gruber, N., Sarmiento, J.L., and Stocker, T.F. (1996) An improved method for detecting anthropogenic CO_2 in the oceans, Global Biogeochem. Cycles, 10, 809-837.

Goyet C., C. Coatanoan, G. Eischeid, T. Amaoka, K. Okuda, R. Healy et S. Tsunogai (1999). Spatial variation of total CO_2 and total alkalinity in the northern Indian Ocean: A novel approach for the quantification of anthropogenic CO_2 in seawater. *Journal of Marine Research,* 57, 135-163.

Hall, Bradley D., Andrew M. Crotwell, Duane R. Kitzis, Thomas Mefford, Benjamin R. Miller, Michael F. Schibig and Pieter P. Tans, (2021), Revision of the World Meteorological Organization Global Atmosphere Watch (WMO/GAW) CO2 calibration scale, *Atmospheric Measurement Techniques*, 14, 4, 3015-3032, 10.5194/amt-14-3015-2021

Keeling, C., J. Chin and T. Whorf, (1996), Increased activity of northern vegetation inferred from atmospheric CO2 measurements, *NATURE*, 382, 6587, 146-149,

Kirk W. Thoning, Pieter P. Tans, Walter D. Komhyr, Atmospheric carbon dioxide at Mauna Loa Observatory: 2. Analysis of the NOAA GMCC data 1974-1985, *Journal of Geophysical Research,* vol.94, 8549-8565 (20 June 1989).

Komhyr, W.D., T.B. Harris, L.S. Waterman, J.F.S. Chin, and K.W. Thoning, Atmospheric carbon dioxide at Mauna Loa Observatory: 1. NOAA GMCC measurements with a non-dispersive infrared analyzer, *Journal of Geophysical Research,* vol.94, 8533-8547 (20 June 1989).

Laika, H.E., Goyet, C., Vouve, F., Poisson, A., Touratier, F., 2009. Interannual properties of the CO_2 system in the Southern Ocean south of Australia. Antarctic Science 21, 663–680. https://doi.org/10.1017/S0954102009990319

Lo Monaco, C. Goyet, N. Metzl, A. Poisson and F. Touratier, 2005. Distribution and inventory of anthropogenic CO_2 in the Southern Ocean: Comparison of three data-based methods. J. Geophys. Res. 110, C09S02. https://doi.org/10.1029/2004JC002571

Morrow R., Donguy J.R., Chaigneau A. and S. Rintoul, 2004. Cold core anomalies at the Subantarctic Front, south of Tasmania.*Deep-Sea Research* I, 51, 1417-1440.

Morrow Rosemary, Kestenare Elodie (2017). 22-year surface salinity changes in the Seasonal Ice Zone near 140°E off Antarctica. *Journal of Marine Systems*, 175, 46-62. https://doi.org/10.1016/j.jmarsys.2017.07.003

Morrow, R., Kestenare, E., 2014. Nineteen-year changes in surface salinity in the Southern Ocean south of Australia. Journal of Marine Systems 129, 472–483. https://doi.org/10.1016/j.jmarsys.2013.09.011

Stephens, B.B., S.C. Wofsy, R.F. Keeling and P. P. Tans, (2000), The CO2 budget and rectification airborne study: Strategies for measuring rectifiers and regional fluxes, *Inverse Methods in Global Biogeochemical Cycles*, Geophy, 114, 311-321,

Tans, P. P., P. S. Bakwin and D. Guenther, (1996), A feasible global carbon cycle observing system: A plan to decipher today's carbon cycle based on observations. *Global change biology*, 2, 3, 309-318,

Touratier, F., Goyet, C., 2004a. Applying the new TrOCA approach to assess the distribution of anthropogenic CO_2 in the Atlantic Ocean. Journal of Marine Systems 46, 181–197. https://doi.org/10.1016/j.jmarsys.2003.11.020

Touratier, F., Goyet, C., 2004b. Definition, properties, and Atlantic Ocean distribution of the new tracer TrOCA. Journal of Marine Systems 46, 169–179. https://doi.org/10.1016/j.jmarsys.2003.11.016

Touratier F., Azouzi L., and C. Goyet (2007). CFC-11, $\Delta^{14}C$, and ^3H tracers as a means to assess anthropogenic CO_2 concentrations in the ocean. Tellus, 59B, 318-325.

Vazquez-Rodrıguez, M., Touratier, F., Monaco, C.L., Waugh, D.W., Padin, X.A., Bellerby, R.G.J., Goyet, C., Metzl, N., Rıos, A.F., Perez, F.F., 2009. Anthropogenic carbon distributions in the Atlantic Ocean: data-based estimates from the Arctic to the Antarctic.

Web references

https://gml.noaa.gov/ccgg/trends/

https://www.icos-cp.eu/

http://www.obs-vlfr.fr/cd_rom_dmtt/sodyf_main.htm

https://scrippsco2.ucsd.edu/data/seawater_carbon/ ocean_time_series.html

https://community.wmo.int/ship-opportunity-programme

https://www.legos.omp.eu/survostral

https://campagnes.flotteoceanogra-phique.fr/series/128/fr/

Data references

https://data.ifremer.fr/SISMER

https:/www.seanoe.org

https:/sss.sedoo.fr